

PID and Hysteresis Current Control for Induction Generator Coupled with Direct Current Motor Fed by Solar Energy System

Omar Talal Mahmood

Mosul Technical Institute, Department of Electrical Technologies, Northern Technical University,
Mosul, Iraq

Abstract: Simulink design for three phase Induction Generator (IG) that is mechanically coupled to separately excited DC motor that supplied from photovoltaic cell has been performed and analysed. A Proportional Integral and Derivative (PID) controller and a hysteresis current controller has been introduced as control techniques to perform a stable performance to the proposed system. The system operation based on controlling the speed of the DC motor to get a suitable value that produces the wanted frequency and voltage values to the 3-phase load from the IG. This is done by using two closed loop control one for the motor speed that fed to PID controller and the other for the motor armature current that fed to the hysteresis current controller to maintain the motor speed within the suitable limit with the aid of DC-DC chopper circuit instead of using the complex three phase inverter circuits. The output voltage and current of the IG is pure sine wave without any harmonics, it is also, a simple power circuit that uses only one switch to control the DC motor armature voltage. This system is reliable if it is used in the isolated power areas and we need only one sensor that is the speed sensor and no need for any extra power source except the solar energy. Step response of the rotor speed for the induction IG has been drawn and analysed. The efficiency of the all system has been calculated, the Total Harmonic Distortion (THD) for the IG voltage and current has been computed using MATLAB Powergui tool, finally, the results has discussed.

Key words: PID induction generator, DC motor, hysteresis current controller, PID, IG, THD

INTRODUCTION

In many applications such as isolated area power generation and medical applications it is needed to generate 3-phase power with a great reliability. Many solutions have been introduced to solve this issue such as the Uninterruptable Power Supplies (UPS). This will need to charge the UPS batteries and the converted solar or wind turbine energy sources has been introduced for this purpose.

Due to diminishing of the conventional fossil energy sources, its harm effect on the environment and global over heating problems, renewable sources (wind, solar, hydro, etc.) has introduced as a very good alternative solution for the energy leakage issue (Ors, 2008). Synchronous generator and induction generator has been used in the renewable generation units but IG has preferred to be used in this units in order to reduce the unit cost, its construction that have no brushes, no need for excitation source and it is easy to have a periodical maintenance, so, it is used widely in the wind turbine plant (Nemmour *et al.*, 2007).

In the wide world, many applications have been introduced to control and generate a cheap and clean

energy using the available wind, solar renewable resources. Chopper circuit has been introduced to control the armature voltage of the DC motor that fed from PV panels, the motor is coupled with water pumping (Rajesh *et al.*, 2014). Speed control strategy has been implemented by Alghuwaieem (1996) to control the DC motor speed that power from solar system which is coupled with 3-phase induction generator to maximize the system efficiency using field current control technique. By Nishida *et al.* (2006) the researchers present a direct control to stand-alone IG using current control structure for bidirectional power flow using pulse width modulation solution.

By Tariq and Yuvarajan (2013) an electronic load controller that supplied from separately excited IG using MATLAB Simulink. Direct couple between photovoltaic solar cell and DC motor (series and shunt excited) has been analysed by Bany (1978) and the motor characteristics were studied. Using Doubly-Fed Induction Generator (DFIG) as a main generator in wind turbine unit provide maximum power and the researchers by Ashish *et al.* (2015) overcome the problem of power oscillation by using novel Adaptive Neuro Fuzzy controller (ANFIS) to control the pitch angle of the IG.

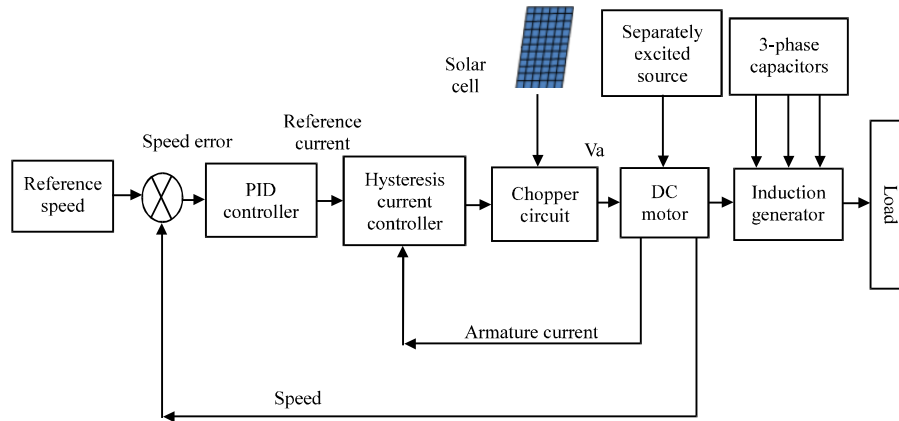


Fig. 1: Control system for the proposed work

MATLAB-Simulink Model has been introduced to simulate the ANFIS (Adaptive Neuro-Fuzzy Inference System) controller that applied to the rotor side converter to control the output power and voltage of a wind system (Syahputra and Soesanti, 2016). Solar cell has been used to run direct current motor using boost converter (Bi-directional DC-DC converter) and a soft switching method has been implemented in MATLAB Simulink Model as a gating signal for the converter switches (Praveen and Mohana, 2014).

Sensorless controller has been designed a low-cost PV pumping system using Permanent Magnet Brushless DC motor (PMBLDC), a boost DC-DC converted is presented to rise the output voltage during the low solar generation during winter period (Kavitha *et al.*, 2004). Finally, a single phase induction motor is fed by solar panels using DC-AC inverter which is coupled with centrifugal pump with an INFOC (Indirect rotor field oriented control) technique is used to get the desired speed for the pump without using DC-DC converter (Feraga and Bouldjedri, 2016).

In the present study, hysteresis current controller has been introduced to generate the gating signal for the Metal Oxide Field Effect Transistor (MOSFET) Switch, the armature current will be fed to the hysteresis current controller and compared with a reference current that produces from PID (Proportional-Integral-Derivative) according to the difference between the desired speed and the actual speed of the separately excited DC motor which is fed by solar panels and mechanically coupled with a 3-phase induction generator. The derive system is consists of solar array, DC-DC converter, PID controller to control the duty cycle of the pulses the hits the gate of the chopper (switch), i.e., the power output of the solar

system is converted to a mechanical power rather than the classical DC-AC converters. The main objective of the proposed system is to convert the electrical power that produced from the solar panels to mechanical power that will derive the IG that will generate a 3-phase smooth and pure sine wave output voltage and current, the proposed system is seen in Fig. 1.

MATERIALS AND METHODS

Theoretical aspects

Hysteresis current control: Current control strategy has been used widely in the power electronic application for generating the gating signals to the power switches to reduce the current error and finally providing a suitable output to derive the plant properly. The simplest current control method is the Hysteresis Current Control (HCC) in which the reference current (generated from PID of PI controller according to speed error for DC motor for example) and the planet current (armature current of the motor) are compared and the error current is ramping up and down between two limits called Hysteresis Band (HB). If the current value become over the upper hysteresis limit, a negative voltage will be fed to the power switch gate to reduce the current (reduces the motor speed as a result) but when the current value falls to the lower hysteresis limit a positive voltage value will applied to the power switch gate to increase current (increases motor velocity in our proposed work) and this cycle will repeated according to the motor speed fluctuation and it is clear in Fig. 2 (Kale and Ozdemir, 2015).

In our research a MATLAB comparator (compare the reference current with the armature current) with relay (with a suitable HD) has been used to produce the

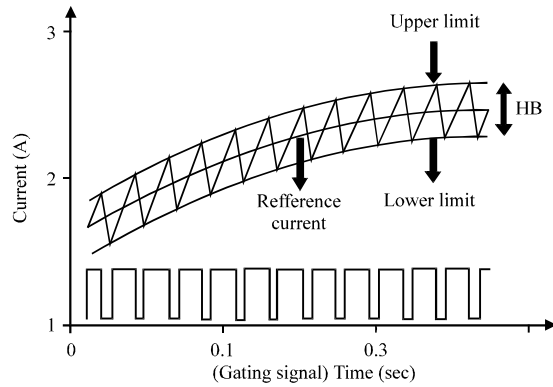


Fig. 2: Hysteresis current control operation wave form

required triggering gate signal as an output of the hysteresis current controller (Le-Huy and Sybille, 2014).

PID controller: This form of controllers is widely used in industrial control process. The PID controller consists of three parameters, proportional gain (K_p), an integration gain (K_i) and a derivative gain (K_d), so, it is important to design the controller to tune these parameters. When the mathematical model of the system can be obtained, it is possible to apply many tuning techniques for determining above gains of the PID controller that will meet the best performance of the closed-loop system (Richard and Robert, 2011).

Ziegler-Nichols rules is the most common tuning method. It can be applied to determine the controller gains with known mathematical models. This method is used here of the mathematical model of the proposed system cannot be derived easily. For this method, there are two manners to obtain the gains in this method which are:

- Method that used the step response
- Method of the stability margin

In our proposed research, we used the second method, first we switch the controller to pure proportional gain increasing the gain continuously until the motor speed shows a permanent oscillation recording the gain value as the critical controller gain K_{cr} , the length of the period P_{cr} (critical period) is measured as in Fig. 3.

From the values of the critical controller gain and length of period it is easy to determine the PID controller gains using Table 1 (Alsammak and Al-Kababji, 2009).

Buck converter circuit: In our research a buck converter has been used to feed the armature circuit of the DC motor with the required operating DC voltage according to the

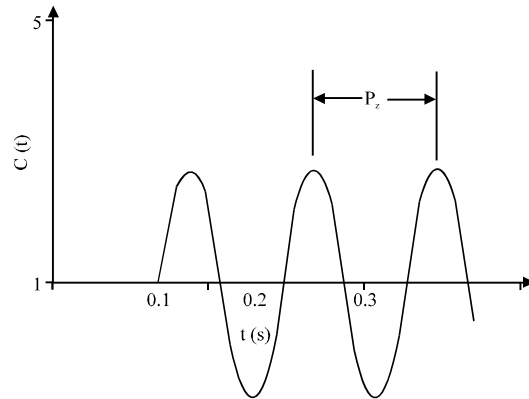


Fig. 3: Evaluation of Pcr

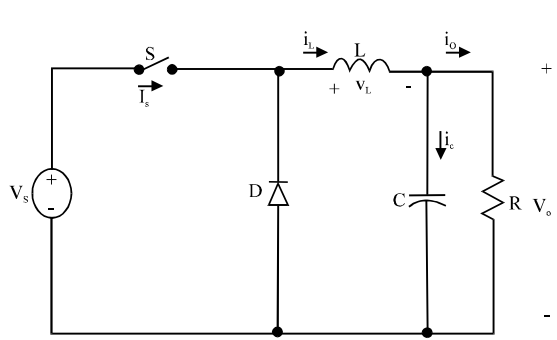


Fig. 4: Circuit diagram for buck converter

Table 1: Ziegler-Nichols tuning rules (second method)

Controller method	K_p	K_i	K_d
P	$0.5 (K_{cr})$	0	0
PI	$0.45 (K_{cr})$	$1.2 (P_{cr})$	0
PID	$0.6 (K_{cr})$	$2 (P_{cr})$	$0.125 (P_{cr})$

gating signals from the HCC circuit that produce the triggering signal to the switch of this converter. Design procedure and calculations has been made to design this converter. The block diagram for this converter is seen in Fig. 4, the inductance and capacitance values can be calculated using the Eq. 1 and 2 (Rashid, 2001):

$$L = \frac{(1-D)R}{Sf} \quad (1)$$

$$C = \frac{(1-D)V_a}{V_{in}Lf^2} \quad (2)$$

Simulation procedures: Figure 5 represents the Simulink program that used in the proposed system, we have the below blocks that are used to form the project:

Separately excited DC motor: In our research, A 220 HP, 500 V armature voltage, 300 V field voltage and 1750 rpm

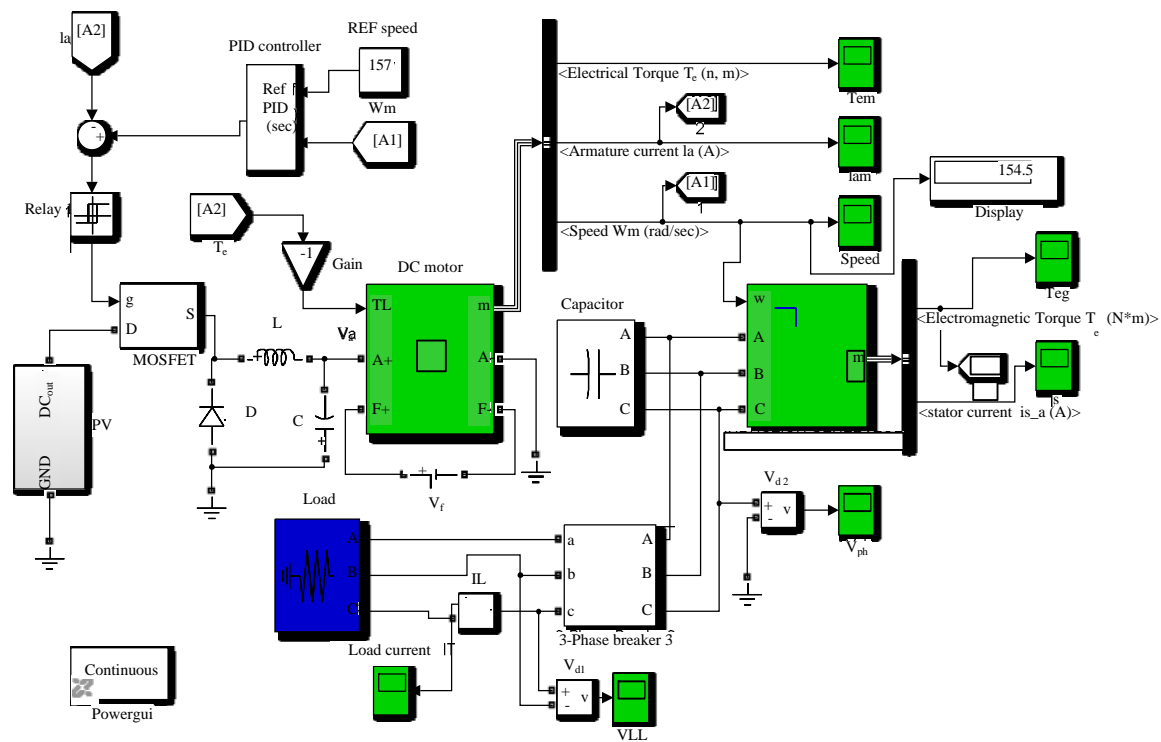


Fig. 5: MATLAB Simulink program for the proposed system.

speed is used. The reference speed of the motor is subjected to 157 rad/sec to give the desired rotor speed of the IG which is an indication to the 50 Hz frequency for the generator outputs. Input voltage for the motor armature circuit is fed from solar cell, the Simulink input for the torque of the motor is selected as T_L and fed from the feedback signal of the electromagnetic torque produced in the induction generator to simulate the load torque input for the motor. The controlled input armature voltage is produced from the chopper circuit and finally the armature controls the input power of the motor, speed of the motor are fed to the hysteresis current controller and the IG, respectively.

Induction generator: In this project, a 215 HP squirrel-cage induction generator has been used with 400 line to line voltage and 50 Hz frequency. Its mechanical input came from the output speed of the DC motor. In the output terminals of the generator, a 3-phased bank capacitor has been connected as self-excitation and a 3-phase 50 kW resistive load is connected via. S-phase breaker which is activated after 2 sec. The measurements of the generator are its output line and phase voltages and the load current.

PID controller: After applying a Ziegler-Nichols tuning rule to the system, the PID gains are obtained. There are two inputs to the PID block, the first came from the motor speed in rad/sec and the second is a constant represents

the reference speed. The output of the controller is represents the reference current that is injected to the next block.

Hysteresis current controller: Two inputs are the Hysteresis current controller block, the first represents reference current came from PID controller and the other one is from the output armature current, these inputs are compared and produce a ramping output that will compared with the reference current via relay which has a parameters (switch on and switch off points) are setting according to the hysteresis band to produce the required wave form that is in Fig. 2. Finally, the output of this controller represents the required gating signals to the chopper circuit that will vary according to the speed fluctuation of the DC motor.

Chopper circuit: Buck converter has been designed to produce the suitable armature voltage that will give the wanted motor speed. This converter consists of MOSFET inductance, capacitance and diode. The design procedures used Eq. 1 to evaluate the value of the inductance and Eq. 2 to evaluate the value of the capacitor of the converter. The converter input is PV cell voltage which is fed to the drain of the MOSFET and the output voltage is the controlled armature voltage from the source of the MOSFET, it will adjust the motor speed to the required value at any load conditions.

RESULTS AND DISCUSSION

Efficiency calculation: Efficiency in general can be calculated as:

$$\eta = \frac{\text{Output power}}{\text{Input power}} \quad (3)$$

The input power of this system is the input power of the separately excited DC motor (P_e) which is:

$$P_e = E_a \times I_2 \quad (4)$$

E_a can be calculated using Eq. 5:

$$E_a = V_a - I_a R_2 \quad (5)$$

Since, R_a of the motor is equal to 0.001986 U, so, we can approximately consider:

$$E_a = V_2$$

So, the input power of the motor is $P_e = V_a \times I_2 = 500 \times 141.1 = 70550$ W. Output power of the generator is:

$$P_{\text{out gen}} = \sqrt{3} \times \text{Line to Line Voltage}(V_{LL}) \times \text{current}(I_{\text{gen}}) \quad (6)$$

From the Simulink module measurements for IG line to line load voltage and current in Fig. 6 and 7, we have the below values for the IG peak current and voltage:

$$V_{LL(m)} = 690 \text{ V and } I_{\text{gen}(m)} = 86.6 \text{ A}$$

$$V_{LL(\text{rms})} = \frac{V_{LL(m)}}{\sqrt{2}} = \frac{690}{\sqrt{2}} = 488 \text{ V}$$

$$I_{\text{gen}(\text{rms})} = \frac{I_{\text{gen}(m)}}{\sqrt{2}} = \frac{86.6}{\sqrt{2}} = 61.16 \text{ A}$$

So that:

$$P_{\text{out gen}} = \sqrt{3} \times 488 \times 61.16 = 51700 \text{ W}$$

$$\eta = \frac{P_e}{P_{\text{out gen}}} = \frac{51700}{70550} = 73.28\%$$

Control parameters calculations: We use Fig. 8, represents the transient response for the speed of the DC motor and from this response it is easy to calculate the step response parameters (Richard and Robert, 2011):

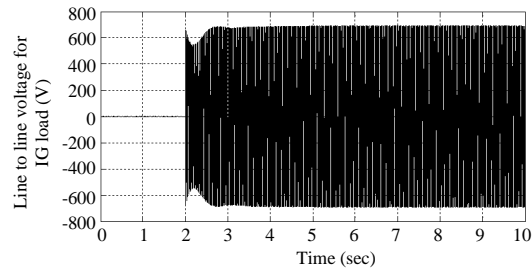


Fig. 6: Line to line voltage for the load of IG

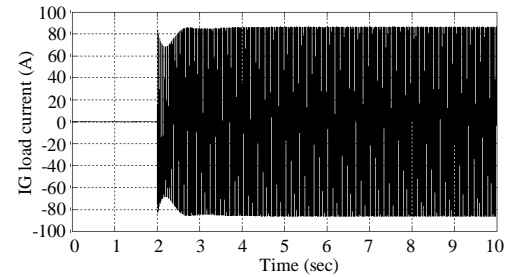


Fig. 7: Load current for the IG

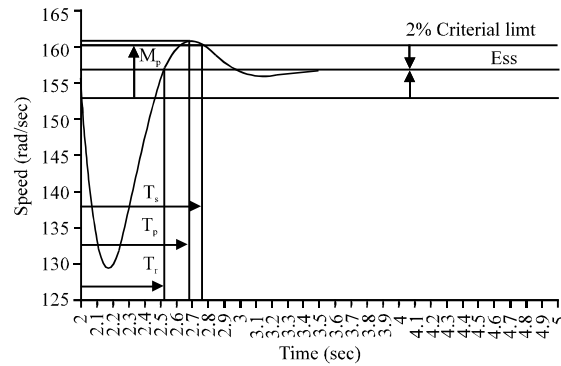


Fig. 8: Step response for speed of DC motor

$$T_p = \frac{\pi}{\omega_n \sqrt{1-\zeta^2}} \quad (7)$$

Time to peak overshoot:

$$T_s = \frac{4}{\omega_n \zeta} \text{ for 2\% criteria} \quad (8)$$

Settling time:

$$M_p = e^{-\pi \zeta / \sqrt{1-\zeta^2}} \quad (9)$$

Maximum percentage overshoots:

$$E_{ss} = e(t) = r(t) - c(t) \quad (10)$$

From Eq. 7 and 8, we calculate the value of ω_n (undamped natural frequency) and ζ (damping ratio) from

Table 2: Control parameters for the proposed PID controller

Type of controller	T_r (sec)	T_p (sec)	T_s (sec)	M_p (%)	E_{ss}	ω_n (rad/sec)	ζ
PID	0.52	0.68	0.76	15.7	0	6.13	0.656

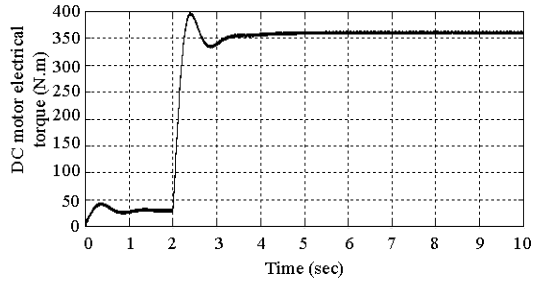


Fig. 9: Electrical torque of DC motor

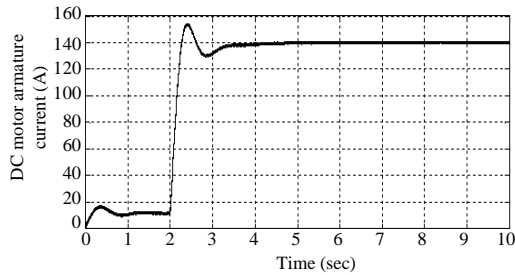


Fig. 10: Armature current of DC motor

Eq. 9 we calculate the value of percentage overshoot ($M_p\%$) and finally it is clear from Eq. 10 that the steady state error for our system is zero. Table 2 represents the result for the control parameters calculations for DC motor step response.

The DC motor electrical torque is shown in Fig. 9, also, the motor armature current is seen in Fig. 10. IG output phase voltage, stator current and electromagnetic torque are in Fig. 11-13, respectively. Finally, the THD analysis results for the IG outputs current and voltages are in Fig. 14a-c.

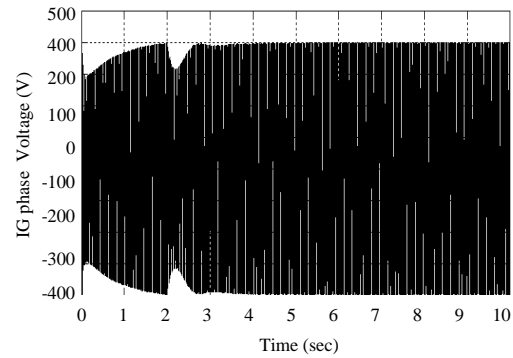


Fig. 11: IG phase voltage

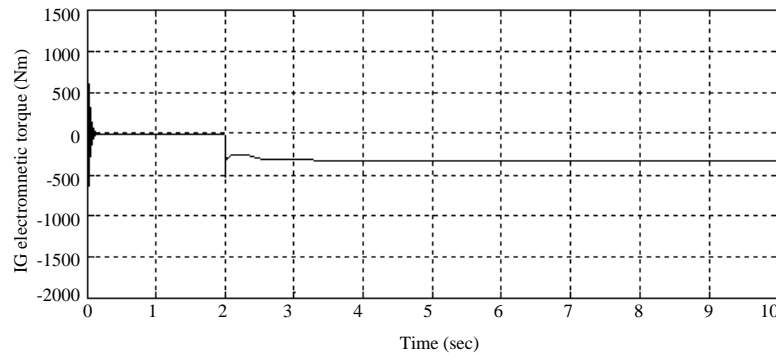


Fig. 12: IG stator phase current

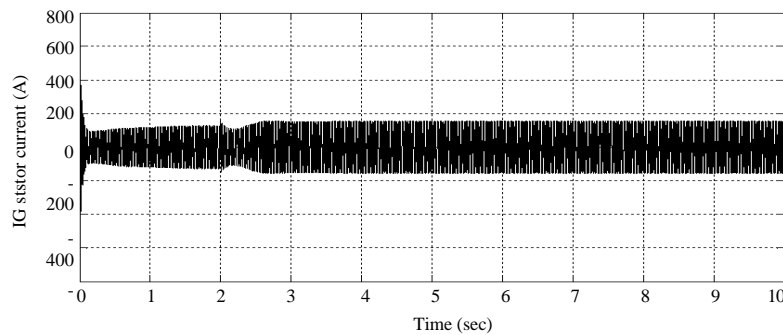


Fig. 13: IG electromagnetic torque

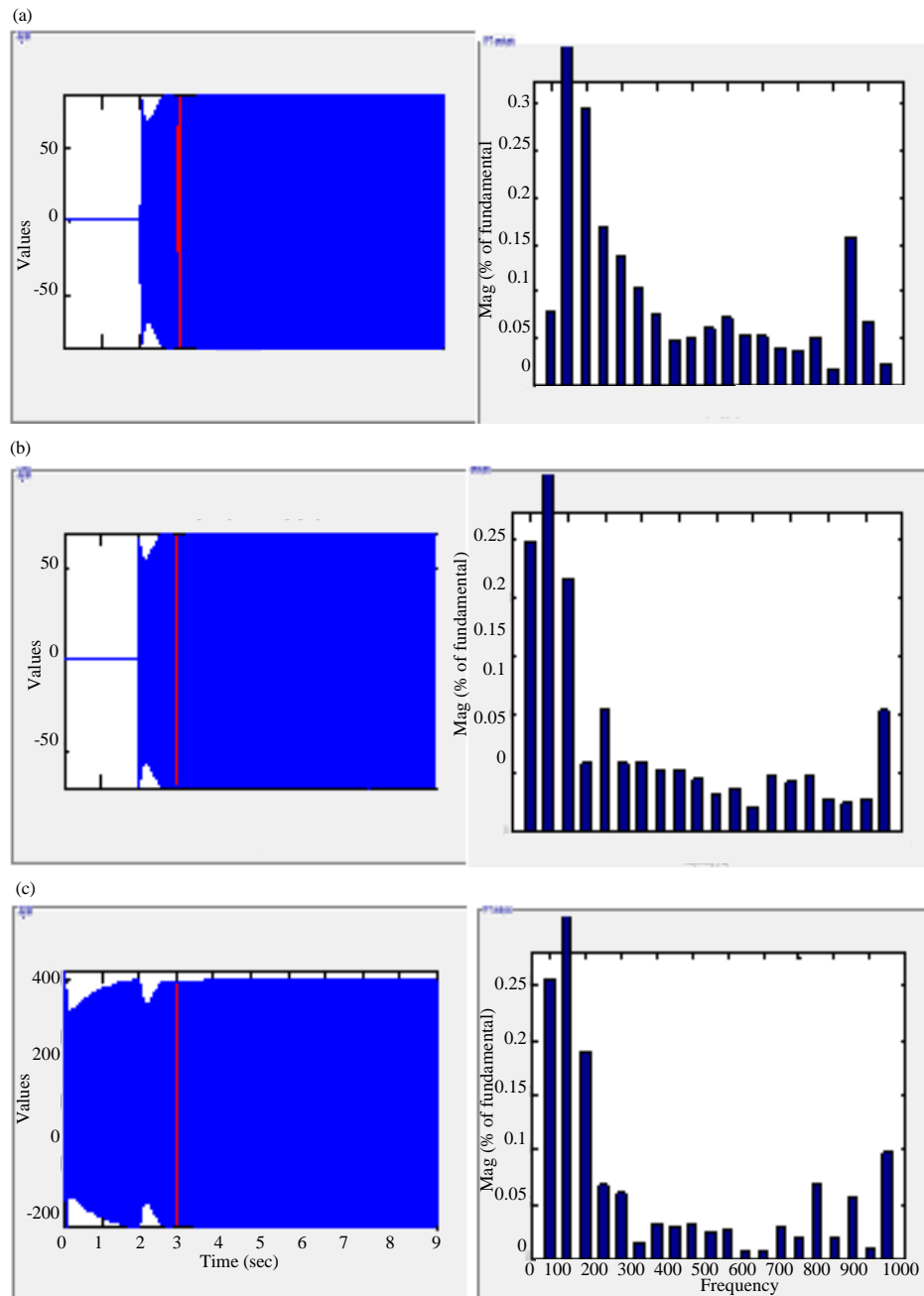


Fig. 15: IG THD analysis for; a) Load current; b) Phase voltage and c) Line to line load voltage; Selected signal: 500 cycles, FFT window (red): 1 cycles, Fundamental (50 Hz) = 84.73, THD = 0.45%; Fundamental (50 Hz) = 674.6, THD = 0.31% Fundamental (50 Hz) = 389.5, THD = 0.26%

CONCLUSION

This project is a simple simulation that subjects a new technique to have an efficient usage of solar energy. In this study, there is a simple control strategy that controls the output voltage and frequency of the IG and produces a pure sine wave for the load current and voltage without

using any filter. From Fig. 15, it is very obvious that THD for the outputs of the IG is very low values and this is an indication to the purity. The speed control for the motor has made simply without any complex technique and the results of the that is illustrated in Fig. 8 and Table 2, indicates that this control method is successful one.as compared with another diesel of gas generation planet,

the proposed plant have a low noise effect, no pollution impact to the environment. Efficiency calculation for this plant indicate 73% which a good efficiency to this cheap method for power generation.

NOTATION

The notation used throughout the study is stated as:

Indexes:

K_p	= Proportional gain
K_i	= Integral gain
K_d	= Derivative gain
P_{cr}	= Critical Period
K_{cr}	= Critical controller gain
η	= Efficiency
P_e	= Input Power for the DC motor (W)
E_a	= Induced voltage in the DC motor Armature (V)
I_a	= Armature current (A)
V_a	= Terminal voltage of the DC motor (V)
R_a	= Armature resistance of the DC motor (Ω)
$P_{out\ gen}$	= Induction generator output power (W)
$V_{LL(rms)}, I_{gen(rms)}$	= IG RMS voltage and current
$V_{LL(m)}, I_{gen(m)}$	= IG peak voltage and current
T_r	= Rise time (sec)
T_p	= Time to peak overshoot (sec)
T_s	= Settling time (sec)
M_p	= Maximum percentage overshoot
ω_n	= Natural frequency (rad/sec)
ζ	= Damping ratio
f	= Switching frequency
D	= Duty cycle
V_{in}	= Input Voltage from solar cell
L, C	= Inductance and Capacitance for buck converter

REFERENCES

- Alghuwainem, S.M., 1996. Speed control of a PV powered DC motor driving a Self-excited 3-phase induction generator for maximum utilization efficiency. *IEEE. Trans. Energy Convers.*, 11: 768-773.
- Alsammak, A.N. and M.F. Al-Kababji, 2009. Reactive power compensation using Fuzzy Gain Scheduling (FGS) based PID controller of synchronous machine. *AL. Rafdain Eng. J.*, 17: 1-24.
- Ashish, K.S., D. Ritesh and S. Dipesh, 2015. Development and simulation of adaptive Neuro Fuzzy controller based pitch angle controlled DFIG system for wind turbine. *Intl. J. Recent Innovation Trends Comput. Commun.*, 3: 3575-3581.
- Bany, J., 1978. Analysis of a direct coupling DC motor and a photovoltaic converter. *Energy Convers.*, 18: 73-79.
- Feraga, C.E. and A. Bouldjedri, 2016. Performance of a photovoltaic pumping system driven by a single phase induction motor connected to a photovoltaic generator. *Automatika*, 57: 163-172.
- Kale, M. and E. Ozdemir, 2015. A new hysteresis band current control technique for a shunt active filter. *Turk. J. Electr. Eng. Comput. Sci.*, 23: 654-665.
- Kavitha, B., S. Karthikeyan and B. Iswarya, 2004. Design of solar PV water pumping system using BLDC drive using sensorless method. *Intl. J. Eng. Sci.*, 3: 41-46.
- Le-Huy, H. and G. Sybille, 2014. Transient analysis of a linear circuit. *Universite Laval, Quebec, Canada*.
- Nemmour, A.L., L. Louze, A. Khezzar and M. Boucherma, 2007. Terminal voltage control of variable speed induction generator driven by a wind turbine supplying a DC load. *Proceedings of the International Conference on Electrical Machines and Power Electronics on Aegean*, September 10-12, 2007, IEEE, Bodrum, Turkey, ISBN:978-1-4244-0890-0, pp: 393-397.
- Nishida, K., T. Ahmed and M. Nakaoka, 2006. A novel induction generator system using Bi-directional PWM converter for Small-scale power applications. *IEEJ. Trans. Electr. Electron. Eng.*, 1: 66-79.
- Ors, M., 2008. Voltage control of a Self-excited induction generator. *Proceedings of the 2008 IEEE International Conference on Automation, Quality and Testing, Robotics (AQTR)* Vol. 3, October 12-15, 2008, IEEE, St. Louis, Missouri, USA., pp: 281-286.
- Praveen, M. and M.R.R. Mohana, 2014. A photovoltaic cell based DC-DC converter for DC motor. *Intl. J. Adv. Res. Electr. Electron. Instrum. Eng.*, 3: 13727-13732.
- Rajesh, R., A. Rahul, P. Mawle and R. Keswani, 2014. PV based chopper fed DC drive. *Proceedings of the International Conference on Industrial Automation and Computing ICIAC*, April 12-13, 2014, Jhulelal Institute of Technology, Lonara, Nagpur, India, pp: 11-16.
- Rashid, M.H., 2001. *Power Electronics Handbook*. 1st Edn., Academic Press, USA., ISBN-13: 9780125816502, pp: 895-635.
- Richard, C.D. and H.B. Robert, 2011. *Modern Control Systems*. 12th Edn., Prentice Hall, Upper Saddle River, New Jersey, USA., ISBN:9780136024583, Pages: 1082.
- Syahputra, R. and I. Soesanti, 2016. DFIG control scheme of wind power using ANFIS method in electrical power grid system. *Intl. J. Appl. Eng. Res.*, 11: 5256-5262.
- Tariq, M. and S. Yuvarajan, 2013. Simulink based modeling, analysis and simulation of self excited induction generator for use in remote areas. *IU. J. Electr. Electron. Eng.*, 13: 1623-1628.